Yan, L., Yu, J., Liu, X., Zhou, K., & Su, B. (2017). The preparation of long-range order lamellar structure porous titanium scaffolds. *Materials Science and Engineering C, 75*, 335-340. https://doi.org/10.1016/j.msec.2016.12.044

The preparation of long-range order lamellar structure porous titanium scaffolds

Leiming Yan[1], Jisi Wu[1], Lei Zhang [*1], Xinli liu[1], Kechao Zhou[1], Bo Su[2]

[1] State Key Laboratory of Powder Metallurgy, Central South University, Changsha 410083, P.R.China

2 School of Oral and Dental Sciences, University of Bristol, Lower Maudlin Street, Bristol BS1 2LY, UK.

ABSTRACT

Porous titanium scaffolds with long-range order lamellar structure were fabricated using a novel bidirectional freeze-casting method. Compared with the ordinarily porous titanium materials made by traditional freeze casting, the titanium walls can offer the structure of ordered arrays with parallel to each other in the transverse cross-sections. And titanium scaffolds with different pore width, wall size and porosity can be synthesized in terms of adjusting the fabrication parameters. As the titanium content was increased from 15 vol.% to 25 vol.%, the porosity and pore width decreased from 67 % to 50 % and 41μm to 32 μm, respectively. On the contrary, as the wall size was increased from 9 μm to 23 μm, the compressive strength and stiffness were increased from 58 ± 8 MPa to 162 ± 10 MPa and from 2.5 ± 0.7 GPa to 6.5 ± 0.9 GPa, respectively. The porous titanium scaffolds with long-range lamellar structure and controllable pore structure produced in present work will be capable of having potential application as bone tissue scaffold materials.

Keywords: Porous titanium, Bidirectional, Lamellar structure, Freeze casting, Mechanical strength

1.Introduction

As a kind of low density and modulus, high strength and good chemical resistance material, titanium is quite suitable for medical implants and other technological applications [1, 2]. For example, when titanium is used as a bone substitute material, the elastic modulus of titanium with a proper level (1~30 GPa) was adjusted to avoid bone resorption and the loosening of the implant [3, 4]. The

increase of porosity is an effective method to reduce the elastic modulus of materials and promotes osteocyte proliferate inside the porous titanium block [5]. The mechanical properties of the materials can be controlled by the porosity, pore size and pore morphology through a variety of manufacturing methods [6]. So far, many manufacturing techniques have been reported to produce porous titanium such as bubble generation [7, 8], replication of polymeric sponge [9, 10], rapid prototyping method [11, 12], space holder method [13, 14] and freeze casting [15, 16].

Freeze casting is a promising method to prepare porous materials with unique aligned and elongated pore structure by driving particles of the slurry to self-assemble along the ice growth direction [6, 17]. The pore morphologies are mainly determined by matrix powder kinds, solvent types and frozen temperature gradient [18]. Generally, matrix powder is divided into two categories: one is ceramic powder, and the other is metal powder. Currently, most of investigations are focused on the ceramic powders, because they can keep stable in the slurry and form obvious layered structure easily compared with metal powders [19]. To get porous metal with uniform layer structure, a certain amount of dispersant and binder were added into slurry to ensure the stable suspension of particles [20]. But the introduction of additives is still difficult to achieve homogeneous distribution for the relatively large titanium particles in the slurry during freeze casting [21]. Currently, the common choice of the solvent to carry powder particles is deionized water and liquid camphene. In the case of camphene-base freeze casting, the highly aligned porous structures with pore sizes over 100 μm could be achieved [22], which can provide enough space for bone ingrowth. However, the metal powder in the slurry is difficult to disperse uniformly during the stage of camphene-based freezing, because it exhibits a tendency to precipitate due to its higher density and larger particle size compared with ceramic powder [23]. Besides, it is difficult to improve the length of the aligned camphene dendrites, because the freezing rate of camphene is slow and the dendrites do not have enough space to grow up [8]. By contrast, when water was used as the freezing vehicle, highly aligned porous structure throughout the entire sample could be achieved [24, 25], and the porous structure can be easily regulated by controlling the

freezing conditions [6, 26]. In addition, water is more suitable as a solvent than liquid camphene, due to its non-toxicity, ordinary and good biocompatibility [27]. Temperature gradient is another important factor for the freeze casting method because it directly controls the process of ice growth. For instance, Yasumasa Chino et al.[26] produced porous titanium material by putting the slurry in an unidirectional temperature gradient field successively to control the directional growth of ice crystal and got long-range aligned pore structure. More importantly, they found the strength and pore morphology of the material was more suitable for implant materials compared with non-directional. The microstructure of the pores can be precisely controlled by this method, however, in particular the lamellar orientation over larger than centimeter dimensions has proven to be difficult. Recently, Robert O. Ritchie et al.[28, 29] have developed a bidirectional freeze casting technique, which was capable of assembling small building blocks into large-sized, single domain, porous lamellar structure, and it displayed an excellent mechanical properties. However, the reported bidirectional freeze casting technique was just restricted to prepare porous ceramic materials.

In present study, we established the possibility of using bidirectional freeze casting method to produce long-range lamellar structure of porous titanium scaffolds. The pore morphology, chemical composition and crystalline structure of the fabricated porous titanium were characterized. Furthermore, we investigated the effects of sintering condition and initial solid content (15, 20, 25 vol.%) on the material structural and mechanical properties.

2.Experimental procedure

The porous titanium scaffolds were produced by controlled freezing of suspension of minute titanium particles. The slurries were prepared by mixing distilled water with a small amount (0.3 wt.% of water) of Xanthan gum dispersant, an organic binder (polyvinyl alcohol, 2 wt.% of the power) and the commercially available titanium powder (15 μm, 99.9 %, China) in various content, depending on the total porosity. Slurries were ball-milled at the rate of 90 rad/min for 24 h with

alumina balls, and then de-aired by string in a vacuum desiccator until air bubbles were completely removed.

Freezing of the slurries was done by pouring them into a square PMMA mould (58×58×50 mm), which bottom was sealed by a PDMS wedge (the slope angle of PDMS wedge is 25°). Thereafter, the mould filled with slurry was placed on the copper cold finger for bidirectional freezing. The slurries with different solid concentrations were frozen under the same experimental temperature (-30 °C) for 6 h to ensure a complete freeze of the slurries. Once freezing was completed, the samples were freeze dried for at least 48 h to ensure a complete removal of the ice crystals in the machine (Pilot2-4M). The rough samples were finally sintered in a vacuum furnace with a digital temperature control system and Mo heating element under a pressure of 1.0×10^{-3} Pa. The green bodies were first heated to 600 °C and held for at least 2 h to make sure a completely removal of the organics. The green bodies were then densified by a high-temperature sintering treatment at a rate of 10 °C/min up to 1200 °C, a steady stage of 2 h at 1200 °C, and keep a cooling rate of 5 °C/min to room temperature.

The structure parameters (pore size, pore shape, thickness of the titanium walls and degree of pore alignment) and chemical compositions of the sintered bodies were characterized by scanning electron microscopy (Nova Nano230, FEI) with energy dispersive spectroscopy (EDS). The phase of the samples was also characterized by X-ray diffraction (D/MAX-RA, Rigaku). The total porosity and open porosity of porous titanium scaffold were determined by the Archimedes method. Compression test have been performed on cube (6×6×6 mm) on an electric servo-hydraulic material Test system (INSTRON 3369), at a constant displacement rate of 2 mm/min. All specimens were used for each experimental condition. The elastic modulus and compressive strength of the samples were measured from the compressive stress-strain curves.

3.Results and discussion

Traditional freeze methods are difficult to precisely control the architectural

features of porous materials with large-size and single-domain. In present work, we introduce a novel freezing technique to obtain porous material to overcome the shortcomings. A schematic diagram of the preparation process is shown in Figure.1. Firstly, the freezing of slurry was poured into a mold, which is placed on top of the copper cold finger covered by a PDMS wedge. Owing to the addition of the wedge, a horizontal temperature gradient was generated during freezing process, which is perpendicular to the vertical temperature gradient. Subsequently, as the slurries began to freeze, the ice crystals formed at the bottom and then began to grow along the dual temperature gradients, and titanium particles were simultaneously pushed by ice crystals into the space between the layers of ice crystals, forming an ice layer alternating with titanium layer structure. Finally, the lamellar ice crystals were then sublimated out, leaving behind a porous titanium scaffold with homogeneous aligned pores. So the porous lamellar titanium structure scaffold with large-sized (centimeter-scale) and single domain were created by the bidirectional freeze casting.

The slurries were bidirectionally frozen at -30 °C, and then the ice crystal was sublimated in a vacuum dry oven for at least 48 h. The titanium particles of green body were pushed together by the PVA, which was separated out from liquid crystals. Fig.2 shows typical SEM images of three directional cross-sections of the unsintered porous titanium scaffold. Fig.2a shows the morphology of transverse cross-sections perpendicular to the direction of the temperature gradient. It is indicated that bidirectional freeze casting can be used to prepare porous titanium scaffold with a long-range aligned lamellar structure. However, it is very difficult to succeed by conventional freeze casting due to the fact that the growth of ice crystals only subjact to unidirectional temperature [24]. Also, it can be seen that there are strong similarity between the as-prepared porous titanium scaffold and lamellar bone in humans [30], which is very important for medical implants. Because the porous titanium scaffolds have 3D feature structure, the complete information of porous titanium scaffolds is limited just from one cross-sectional image. To possess an overall understanding for the structure of porous materials, Fig.2b and Fig.2c present the morphology of mutually perpendicular longitudinal cross-sections of the sample, which is

significantly different. The surface of the titanium walls is not absolutely smooth in practice, but has long edge aligned distribution on it throughout the whole sample along the temperature gradient, as shown in Fig.2b. The reason why the surface morphology was rough could be attributed to directional growth of ice dendrites that drive titanium particles directional movement. These sheet-like ice dendrites which ranked neatly on the surface of titanium walls continue to grow, and pushed titanium powders together slowly. That led to the formation of long ledge between the two ice dendrites. We can also call the long edge as “titanium bridges” that connects between the layers. The lamellar structure also can be clearly seen from Fig.2c, which was parallel to the temperature gradient and perpendicular to the titanium walls.

In the process of sintering, the porous titanium scaffolds may change the structure morphology with increasing temperature, and it can also form a new phase due to pure titanium with high chemical activity, which easily reacts with other elements(C, O, et al.) at high temperature. The new phase has a strong detrimental effect on the mechanical properties of porous titanium, therefore controlling the sintering atmosphere is very important to porous titanium scaffold. Fig.3 shows the typical SEM figures of the sintered specimen containing 20 vol.% of initial solid content. Comparing with the structure of green bodies, as shown in Fig.2, there was no obvious variation for the uniform lamellar structure of sintered specimen. It is indicated that the sintering had little effect on the pore morphology of the sample. The sintering process mainly affected the density of the sample rather than pore configuration. To carefully observe the structure of porous titanium scaffold, an amplification image was given, as shown in the Fig.3b, which transverse cross-sections is parallel to the temperature gradient. It is obvious that the walls of porous titanium scaffolds had high density, arranged paralleled with each other and not obvious micro-pores. The titanium bridge, which connected two titanium walls, can be seen clearly, and it was evenly distributed across all the layers. The surface of titanium walls (Fig.3c) was also very rough due to the existence of titanium bridges on the plane after being sintered. Because of the existence of titanium bridges between the layers, the strength of porous titanium material was improved.

The chemical compositions of the samples were characterized by XRD and EDS. The typical XRD pattern of the sample sintered at 1200 °C with an initial titanium content of 20 vol.% is shown in Fig.4. The sintered sample only showed peaks related with the crystalline titanium phase (JCPDS: 44-1294), which demonstrated that the titanium powder did not generate vigorous reaction with C and O in the process of specimens preparation. Fig.5 shows a typical EDS spectrum of the sample with initial titanium content of 20 vol.%. Corresponding to the strong peaks of titanium metal were observed and any noticeable secondary elements has not been found, which demonstrated that the sample prepared by the above route has pure Ti phases. In addition, the possible impurities of sample were examined using an elemental analyzer. The oxygen content of raw titanium powders is 1.13 %, and it had been increased to 1.72 % after vacuum sintering, that was higher than the critical value which can deteriorate the ductility of titanium metal [15]. The same variation tendency had been displayed in carbon content, which is increased from 0.03 % to 0.51 %. As analyzed from above, it is obvious that the increase of impurity content is less than 0.8 %. This suggests that the impurity contents of the final sample were mainly from the raw titanium particles, which increased the size of the powders to reduce impurity contamination.

When sintering temperature is same, the initial solid content is a major factor to adjust the porosity and influence pore structure [31]. Therefore, the study on the relation between them is extremely essential. Fig.6a-c shows the SEM images of the porous titanium scaffolds produced with various initial titanium contents (15, 20, and 25 vol.%). Regardless of the titanium content, all the fabricated samples with the uniform elongated pores are achieved. With the increase of initial solid content (from 15 to 25 vol.%), the porosity decreased, the titanium wall became massively thicker, the pore width became smaller, while the number of titanium bridges did not show a clear change. The main reason is that the ice crystals have wider space to nucleate and grow with the decrease of solid content in slurry. Table 1 lists the porosity, wall size and pore width of the fabricated samples with various initial titanium contents. The porosity decreased from 67 % to 50 % with the enhancement of titanium content from

15 to 25 vol.%; the wall size and the pore width increased from 9 to 23 μm and decreased from 41 to 32 μm, respectively. The open-cell rate of all the samples is over 80 %. Interestingly, according to these data, a simple formula can be used to quantitatively analyze the porosity and structure parameters (wavelength, wall size and the size of titanium bridges) of porous titanium scaffold as follows:

$$p = 100(1 - \frac{\delta_w + \delta_b}{\lambda}) \quad \text{（1）}$$

where, p is the porosity percentage, λ is the wavelength of the structure[32], δ_w is the wall size of porous titanium scaffold, δ_b is the size of titanium bridge between layers. For this particular structure, the new calculation formula of porosity can be used.

In general, the total porosity of titanium scaffolds was greater than 50 %, which made that the bone cells might be more prone to grow into the pores. As a suitable medical implant material, there is not only sufficient porosity, but also enough strength to satisfy the safety and stability under the certain load. However, the mechanical properties are sharply decreased with the increase of porosity. Therefore, the balance between the porosity and mechanical properties of titanium scaffolds should be further investigated [6, 33].

Due to the fact that the bone mainly bears unidirectional compressive stress during exercise, the compressive property of the materials is tested and to evaluate whether it will work for organisms [34]. Typical engineering stress-strain curves were obtained by compression testing of porous titanium samples with aligned pores, including the samples with three kinds of different initial solid content, as shown in Fig.7. Basically, all the fabricated samples exhibited the typical fracture behavior of metallic porous scaffolds. In other words, three distinctive regions: the linear elastic response, yield segments and plastic deformation stage were observed. During the elastic deformation phase, the stress-strain curves basically presents an upward tendency in a straight line, and the slope of the curve is associated with elastic modulus that is most important parameters to judge the implant materials generate stress shielding. With the increase of deformation, the porous titanium material did not produce obvious yield stage, only a yield point, namely the compression strength.

As expected, given the high oxygen content of the titanium, which is beyond the value of ~0.8 wt.% O resulting in near-zero tensile ductility in titanium. Besides, beyond the yield point, the stress-strain curves suddenly became very twisting. This is due to the fact that porous titanium scaffold with the unique long-range lamellar structure was obtained, which generated stress concentration in the internal titanium walls with the expansion of the crack that parallel to the layer.

Fig.8 presents the compressive strengths and stiffness of the porous titanium scaffolds with various initial titanium contents (15, 20, and 25 vol.%). The compressive strength increased considerably from 58 ± 8 to 162 ± 10 MPa with an increase in titanium content from 15 to 25 vol.%, and the compressive stiffness increased remarkably from 2.5 ± 0.7 to 6.5 ± 0.9 GPa. These increases in compressive strength and stiffness are mainly attributed to the decrease in the porosity of the sample. Moreover, it should be noted that the compressive strength is 15~20 % higher than the traditional porous titanium scaffolds prepared by ourselves at the same porosity, and further prove the view by comparing the unidirectional freeze casting has been reported by Dvaid [35]. In addition to superior compressive strength, the stiffness is much lower than the critical value of 30 GPa to avoid the bone resorption caused by stress shielding, which is beneficial for bone repair.

4. **Conclusions**

Highly porous titanium scaffolds with a long-range aligned lamellar structure were successfully fabricated by bidirectional freeze casting of aqueous slurries of titanium powders, followed by freeze drying to remove ice dendrites and sintering to density the powders into continuous walls. The main results can be summarized as follows:

(1) Compared with the sample before sintering, microstructure analysis reveals the pores which aligned and sheet-like produced by removal of the ice dendrites had not significant change after heat treatment. In addition, the increase of the impurity contents of the final sample relatively low, which the main increased oxygen content is lower than 0.8 wt.% where titanium becomes brittle in tension. The impurity

contents of raw titanium powder increase with the powder size, therefore, controlling the powder size is the key factor to improve the mechanical properties of porous titanium scaffolds.

(2) As the titanium content increased from 15 to 25 vol.%, the porosity of titanium scaffolds decreased from 67 to 50 %. And the pores were aligned along the freeze direction and their wall-to-wall distance varied with the initial titanium content, in accordance with theoretical considerations.

(3) The compressive strength and stiffness increased from 58 ± 8 to 162 ± 10 MPa and from 2.5 ± 0.7 to 6.5 ± 0.9 GPa, respectively. Compared with the materials created by traditional freeze casting, porous titanium scaffolds prepared by bidirectional freeze casting show more excellent mechanical property and environment for bone repair, so it is a very promising material for bone tissue engineering applications.

Acknowledgments

This research was supported by the National Nature Science Foundation of China (No.51674304, 51604305), China Postdoctoral Science Foundation (2016M592445) and the Postdoctoral Science Foundation of Central South University.

References:

[1] D.T. Queheillalt, H.N. Wadley, B.W. Choi, D.S. Schwartz, Creep expansion of porous Ti-6Al-4V sandwich structures, Metallurgical and Materials transactions A 31 (2000) 261-273.

[2] X. Liu, P.K. Chu, C. Ding, Surface modification of titanium, titanium alloys, and related materials for biomedical applications, Materials Science and Engineering: R: Reports 47 (2004) 49-121.

[3] G. Ryan, A. Pandit, D. Apatsidis, Fabrication methods of porous metals for use in orthopaedic applications, Biomaterials 27 (2006) 2651-2670.

[4] G.H. Van Lenthe, M.C. de Waal Malefijt, R. Huiskes, Stress shielding after total knee replacement may cause bone resorption in the distal femur, Bone and joint journal 79 (1997) 117-122.

[5] A. Bignon, J. Chouteau, J. Chevalier, G. Fantozzi, J.P. Carret, Effect of micro- and macroporosity of bone substitutes on their mechanical properties and cellular response, Journal of Materials Science Materials in Medicine 14 (2003) 1089-1097.

[6] S. Deville, Freeze-Casting of Porous Biomaterials: Structure, Properties and Opportunities, Materials 3 (2010) 1913-1927.
[7] Z.X. Guo, C. Jee, N. Özgüven, J. Evans, Novel polymer–metal based method for open cell metal foams production, Mater. Sci. Tech-lond 16 (2000) 776-780.
[8] Y. Higuchi, Y. Ohashi, H. Nakajima, Biocompatibility of Lotus–type Stainless Steel and Titanium in Alveolar Bone. Adv. Eng. Mater. 8 (2006) 907-912.
[9] S.R. Frenkel, W.L. Jaffe, F. Dimaano, K. Iesaka, T. Hua, Bone response to a novel highly porous surface in a canine implantable chamber, Journal of Biomedical Materials Research Part B: Applied Biomaterials 71(2004) 387-391.
[10] B. Levine, A new era in porous metals: applications in orthopaedics, Adv. Eng. Mater. 10 (2008) 788-792.
[11] W. Xue, B.V. Krishna, A. Bandyopadhyay, S. Bose, Processing and biocompatibility evaluation of laser processed porous titanium, Acta. Biomater 3 (2007) 1007-1018.
[12] L. Mullen, R.C. Stamp, W.K. Brooks, E. Jones, C.J. Sutcliffe, Selective Laser Melting: A regular unit cell approach for the manufacture of porous, titanium, bone in-growth constructs, suitable for orthopedic applications, Journal of Biomedical Materials Research Part B: Applied Biomaterials 89 (2009) 325-334.
[13] C.E. Wen, M. Mabuchi, Y. Yamada, K. Shimojima, Y. Chino, Processing of biocompatible porous Ti and Mg, Scripta Materialia 45 (2001) 1147-1153.
[14] T. Imwinkelried, Mechanical properties of open-pore titanium foam, Journal of Biomedical Materials Research Part A 24 (2007) 964-970.
[15] Y. Chino, D.C. Dunand, Directionally freeze-cast titanium foam with aligned, elongated pores, Acta. Mater. 56 (2008) 105-113.
[16] S. Yook, B. Yoon, H. Kim, Y. Koh, Y. Kim, Porous titanium (Ti) scaffolds by freezing TiH2/camphene slurries, Mater. Lett. 62 (2008) 4506-4508.
[17] S.E. Naleway, K.C. Fickas, Y.N. Maker, M.A. Meyers, J. McKittrick, Reproducibility of ZrO2-based freeze casting for biomaterials, Materials Science and Engineering: C 61 (2016) 105-112.
[18] M.M. Porter, R. Imperio, M. Wen, M.A. Meyers, J. McKittrick, Bioinspired Scaffolds with Varying Pore Architectures and Mechanical Properties, Adv. Funct. Mater. 24 (2014) 1978-1987.
[19] H. Jung, S. Yook, H. Kim, Y. Koh, Fabrication of titanium scaffolds with porosity and pore size gradients by sequential freeze casting, Mater. Lett. 63 (2009) 1545-1547.
[20] S. Deville, Freeze-Casting of Porous Ceramics: A Review of Current Achievements and Issues, Adv. Eng. Mater. 10 (2008) 155-169.
[21] H. Jung, S. Yook, T. Jang, Y. Li, H. Kim, Y. Koh, Dynamic freeze casting for the production of porous titanium (Ti) scaffolds, Materials Science and Engineering: C 33 (2013) 59-63.
[22] B. Yoon, W. Choi, H. Kim, J. Kim, Y. Koh, Aligned porous alumina ceramics with high compressive strengths for bone tissue engineering. Scripta Mater, 58 (2008) 537-540.
[23] Y. Soon, K. Shin, Y. Koh, W. Choi, H. Kim, Assembling unidirectionally frozen alumina/camphene bodies for aligned porous alumina ceramics with larger dimensions, J. Eur. Ceram Soc. 31 (2011) 415-419.
[24] S. Deville, E. Saiz, A.P. Tomsia, Freeze casting of hydroxyapatite scaffolds for bone tissue engineering. Biomaterials 27 (2006) 5480-5489.
[25] Q. Fu, M.N. Rahaman, F. Dogan, B.S. Bal, Freeze casting of porous hydroxyapatite scaffolds.

I. Processing and general microstructure, Journal of Biomedical Materials Research Part B: Applied Biomaterials 86 (2008) 125-135.
[26] Y. Chino , D.C. Dunand, Directionally freeze-cast titanium foam with aligned, elongated pores, Acta. Mater. 56 (2008) 105-113.
[27] S. Yook, H. Jung, C. Park, K. Shin, Y. Koh, Y. Estrin, H. Kim, Reverse freeze casting: A new method for fabricating highly porous titanium scaffolds with aligned large pores, Acta. Biomater. 8 (2012) 2401-2410.
[28] H. Bai, Y. Chen, B. Delattre, A.P. Tomsia, R.O. Ritchie, Bioinspired large-scale aligned porous materials assembled with dual temperature gradients, Science advances 1 (2015).
[29] H. Bai, F. Walsh, B. Gludovatz, B. Delattre, C. Huang, Y. Chen, A. Tomsia, R. Ritchie, Bioinspired Hydroxyapatite/Poly(methyl methacrylate) Composite with a Nacre-Mimetic Architecture by a Bidirectional Freezing Method, Adv. Mater. 28 (2016) 50-56.
[30] U.G. Wegst , H. Bai, E. Saiz, A.P. Tomsia, R.O. Ritchie, Bioinspired structural materials, Nat. Mater. 14 (2015) 23-36.
[31] M.J. Jrgensen, S. Primdahl, C. Bagger, M. Mogensen, Effect of sintering temperature on microstructure and performance of LSM–YSZ composite cathodes, Solid State Ionics 139 (2001) 1-11.
[32] S. Deville, E. Saiz, A.P. Tomsia, Ice-templated porous alumina structures. Acta. Mater. 55 (2007) 1965-1974.
[33] T.M. Freyman, I.V. Yannas, L.J. Gibson, Cellular materials as porous scaffolds for tissue engineering. Prog. Mater. Sci. 46 (2001) 273-282.
[34] M.C.T. Asuncion, J.C. Goh, S. Toh, Anisotropic silk fibroin/gelatin scaffolds from unidirectional freezing, Materials Science and Engineering: C 67 (2016) 646-656.
[35] J.C. Li, D.C. Dunand, Mechanical properties of directionally freeze-cast titanium foams. Acta. Mater. 59 (2011) 146-158.

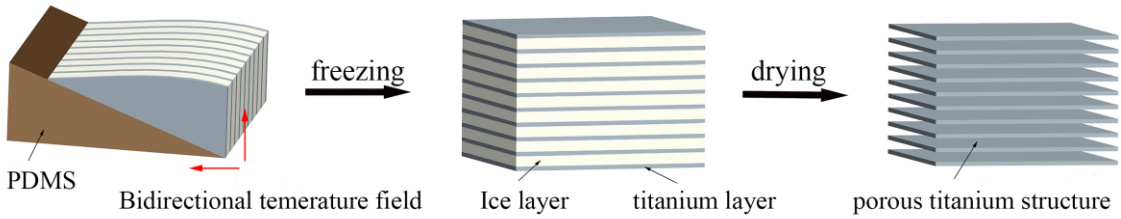

Fig.1. Schematic diagram showing the creation of long-range lamellar structure of porous titanium scaffolds using bidirectional freeze casting.

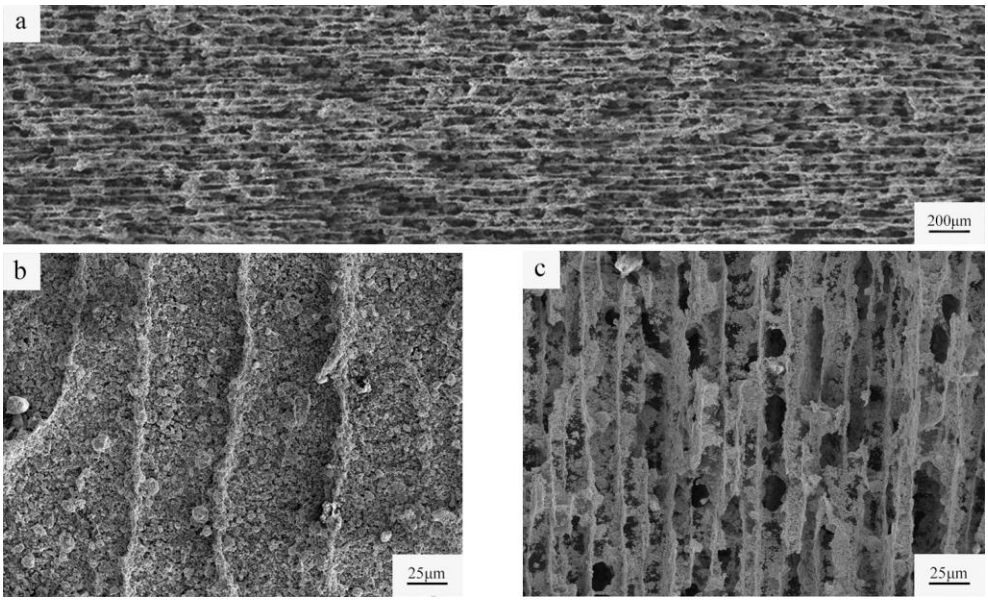

Fig.2. SEM images of porous titanium scaffold prepared by bidirectional freezing before sintered. (a) showing the morphology of transverse cross-section perpendicular to the temperature gradient; (b) showing the titanium walls surface morphology; (c) showing the longitudinal cross-section formed 90 degree angles with (b).

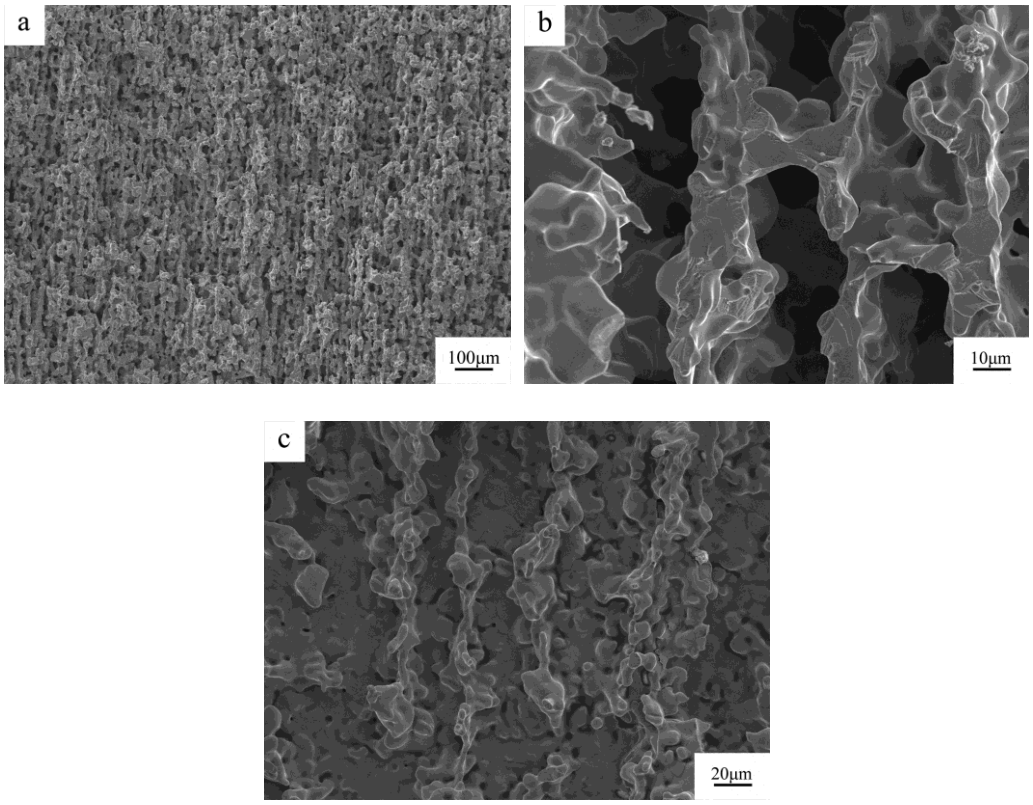

Fig.3. SEM images of porous titanium scaffold prepared by bidirectional freezing after sintered. (a and b) showing the longitudinal cross-sections with low and high magnification respectively; (c) showing the titanium walls surface morphology.

Table 1 porosity, wall size and pore width of the porous Ti scaffolds produced with various initial Ti contents (15, 20, 25 vol.%).

Initial solid loading (vol.%)	15	20	25
Porosity (%)	67	59	50
Wall size (μm)	9	15	23
Pore width(μm)	41	35	32

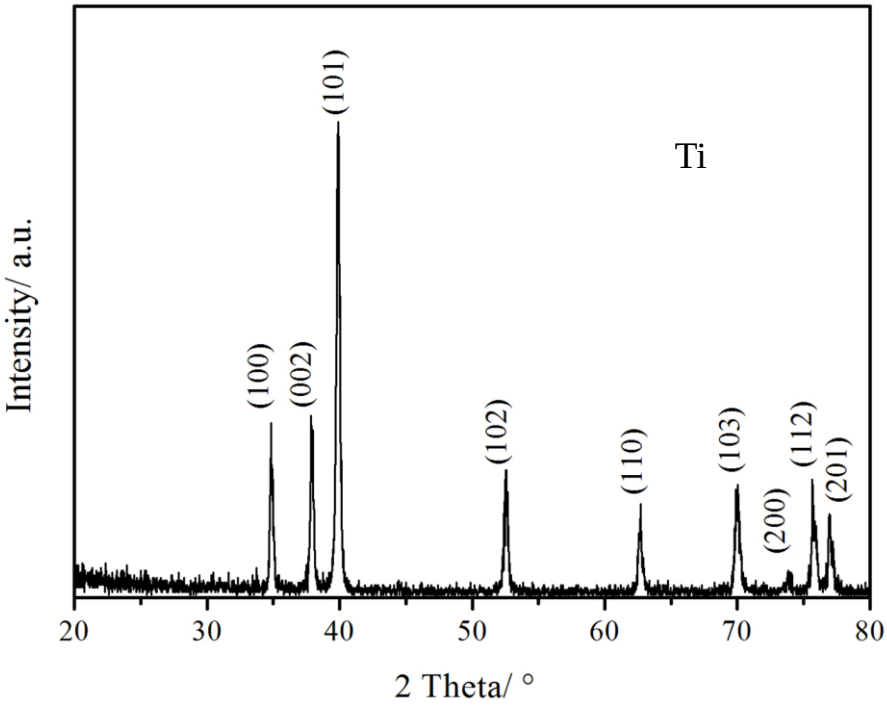

Fig.4.Typical X-ray diffraction patterns of the sintered sample with an initial titanium content of 20 vol.%.

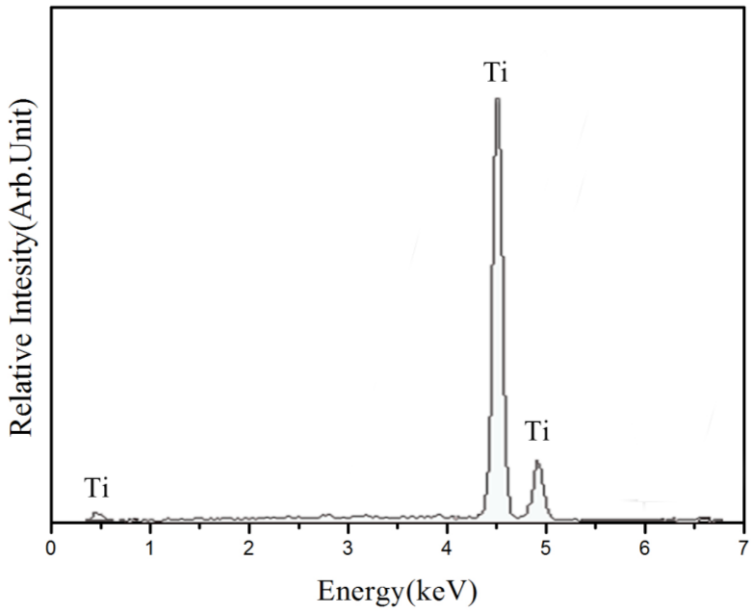

Fig.5. Typical EDS spectrum of the porous Ti scaffold produced with an initial titanium content of 20 vol.%.

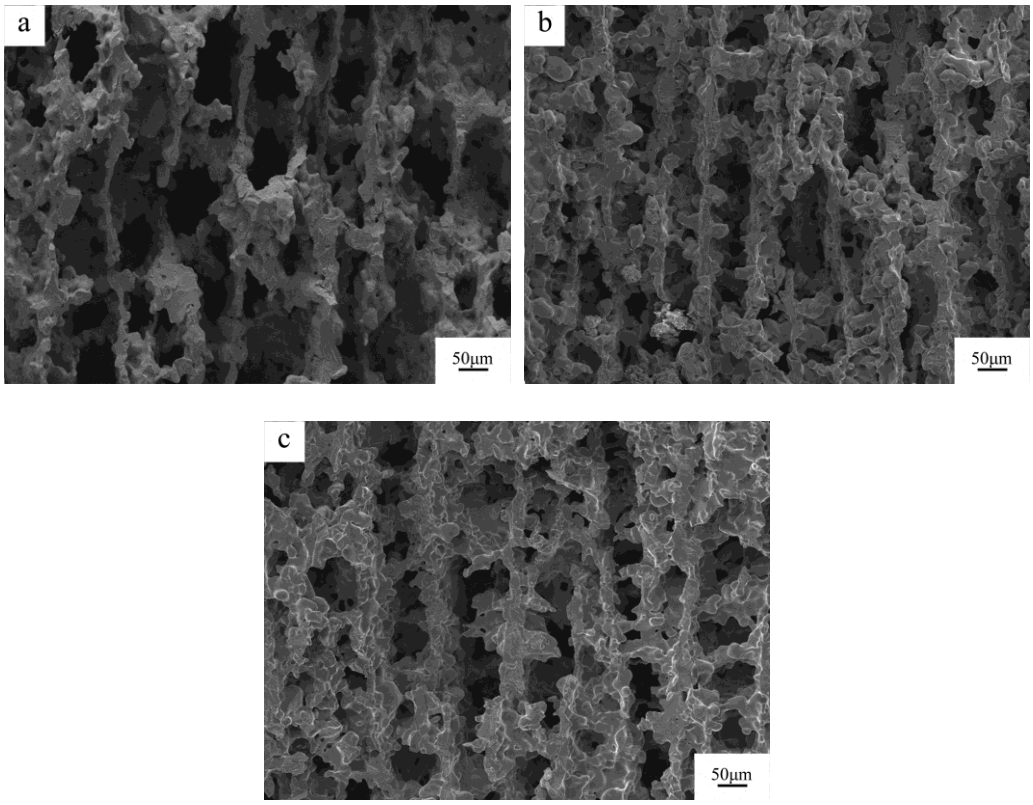

Fig.6.SEM images of the porous Ti scaffold Ti scaffolds produced with various initial Ti contents of 15 (a), 20 (b), and 25 vol.%(c).

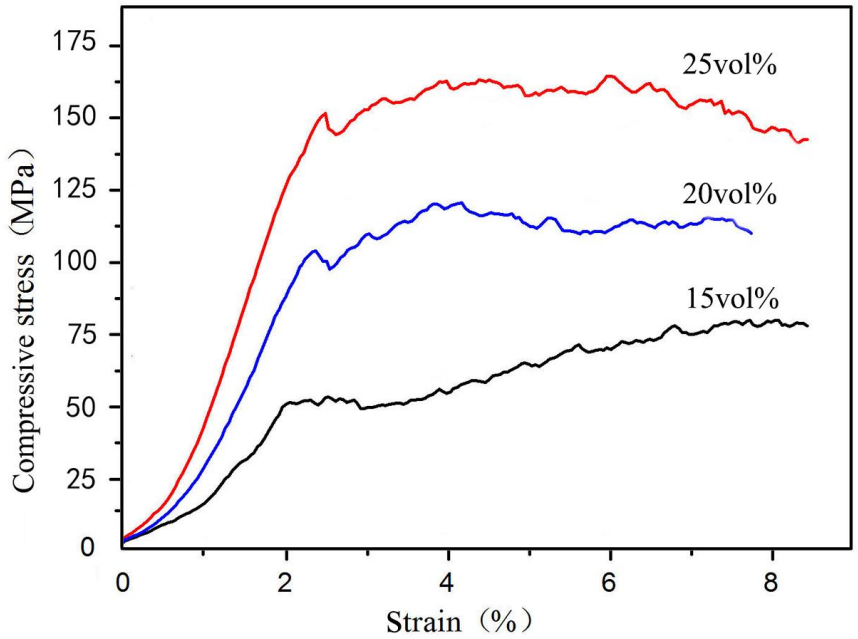

Fig.7. Typical compressive stress versus strain responses of the porous titanium scaffolds produced with various initial titanium content (15, 20, and 25 vol.%).

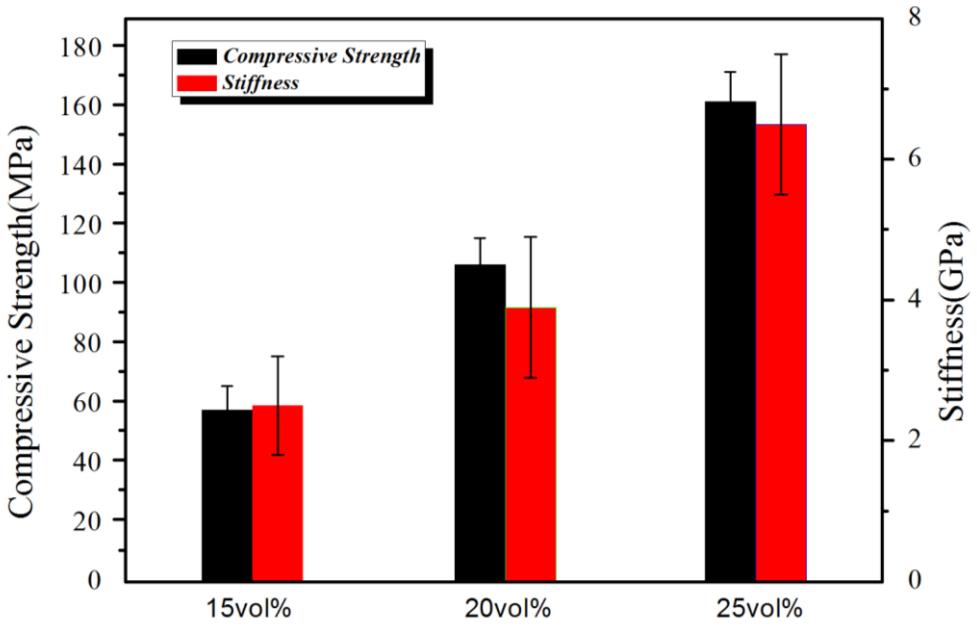

Fig.8. Compressive strength and stiffness of the porous titanium scaffolds as a function of the initial titanium content.